1

Bridged Lactams as Model Systems for Amidic Distortion

Tyler J. Fulton, Yun E. Du, and Brian M. Stoltz

California Institute of Technology, Division of Chemistry and Chemical Engineering, Pasadena, California, 91125, United States

1.1 Introduction and Scope

Amide linkages are pervasive functional groups present in peptides, natural products, and bioactive materials [1]. The high degree of resonance contribution of the amide nitrogen n_N to $\pi^*_{C=O}$ (15–20 kcal/mol stabilization from resonance form **2**, Scheme 1.1) imparts approximately 40% double bond character and renders typical amides planar and less reactive toward nucleophilic attack compared with other carbonyls and carboxylic acid derivatives (Scheme 1.1) [2]. Disruption of the n_N to $\pi^*_{C=O}$ resonance via distortion of the amide bond is a mode of amide activation with a rich history dating back to the l938 when Lukeš first proposed that incorporation of an amide nitrogen into the bridgehead position of a bicyclic system would be "sterically impossible" and violate Bredt's rule [3]. Lukeš further hypothesized that if amides bearing a bridgehead nitrogen were successfully synthesized, they would bear properties more akin to those of ketones. Bridged lactams have since served as a remarkable tool for the understanding of the amide bond and its properties. This chapter provides a review of bridged lactams up to 2020. A comprehensive discussion of bridged lactams is outside of the scope of this entry; therefore, the present chapter is focused on the reactivity and properties of bridged lactams as models for amidic distortion. The most recent comprehensive review of bridged lactams was published by Szostak and Aubé in 2013 [4], with an update of the field covering the period of 2014–2018 from Szostak [5]. For a full accounting of the synthesis of bridged lactams, we direct the reader to these recent reviews [4, 5].

The nomenclature and classifications of twisted amides were originally delineated by Yamada [6] and have become standard for discussion within the field [7]. Destabilization of amide resonance **2** can be affected by several general means: intramolecular steric repulsion, intramolecular steric restriction, intermolecular steric restriction, electronic delocalization (e.g. classical anomeric amides), and conformational effects (Figure 1.1) [4]. It is important to note that *destabilized amide* is a more general term, whereas *nonplanar amide* refers specifically to an amide that has been geometrically destabilized via steric and/or electronic factors, i.e. the

Amide Bond Activation: Concepts and Reactions, First Edition. Edited by Michal Szostak.

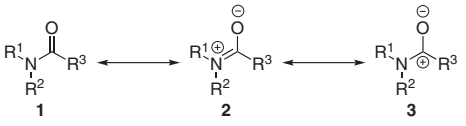

Scheme 1.1 Resonance structures of the amide bond.

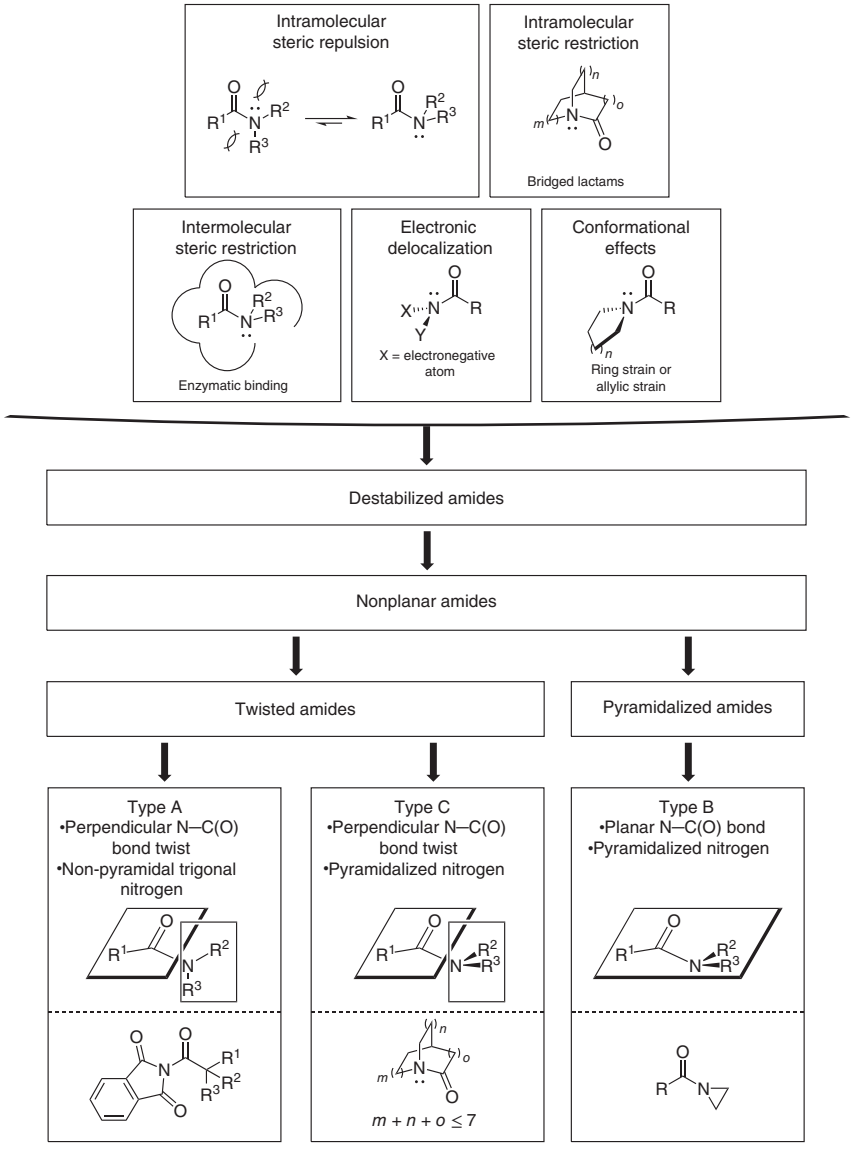

Figure 1.1 Amidic distortion and types of nonplanar amides.

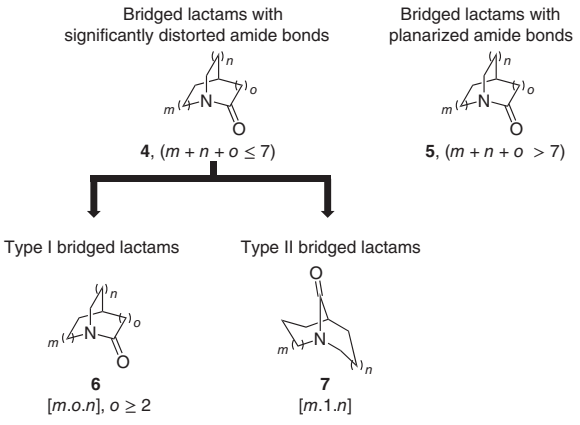

Figure 1.2 Types of bridged lactams.

contribution of resonance form **2** has been diminished. Qualitatively, nonplanar amides can be divided into Types A, B, and C as described by Yamada [6]. Type A amides contain a perpendicularly twisted N–C(O) bond with a nonpyramidalized trigonal geometry at nitrogen. Type B amides contain a significant pyramidalization of the nitrogen atom with a planar N–C(O) bond geometry. Type C amides are a combination of Type A and Type B wherein the N–C(O) bond is twisted with a pyramidalized nitrogen. Both Type A and Type C amides are known as *twisted amides*, while Type B amides are known as *pyramidalized amides*.

Bridged lactams represent one specific class of nonplanar twisted amides wherein the amide nitrogen is embedded in the ring fusion of a bridged bicyclic scaffold, consequently resonance form **2** constitutes an anti-Bredt double bond in a bridged lactam. Steric restriction of the amide bond in such a way remains the most successful strategy by far for distortion of the amide bond. Bridged lactams therefore constitute privileged chemical motifs for understanding the structure and reactivity of distorted amide bonds in general [8]. In addition to the insights into the nature of the amide bond, amidic distortion is critical for understanding cis/trans-isomerization in peptides for protein folding [9]. Bridged lactams are divided into Type I scaffolds where the N–C(O) bond is on a bridge consisting of two or more carbon atoms or Type II where the N–C(O) bond is on a single carbon bridge (Figure 1.2). Type II bridged lactams are generally more strained than the corresponding Type I bridged lactams; however, they tend to be more resistant to hydrolysis due to medium ring scaffolding effects [10]. Bridged lactams wherein the 1-azabicyclo core contains more than 10 atoms will not be covered as these structures display physical properties and reactivity akin to that of planar amides.

1.2 General Properties of Bridged Lactams

1.2.1 Parameters of Amide Bond Distortion

The Winkler–Dunitz distortion parameters provide a quantitative assessment of amide bond distortion based on the twist angle (τ), *N*-pyramidalization (χ_N),

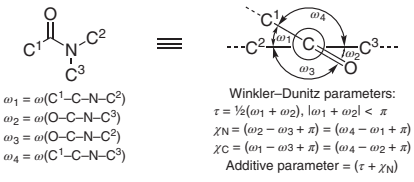

Figure 1.3 Winkler–Dunitz parameters for quantitative assessment of amide bond distortion.

and *C*-pyramidalization (χ_C) (Figure 1.3) [11]. The twist angle τ describes the magnitude of rotation about the N–C(O) bond. Quantitatively, τ is 0° for a planar amide bond and 90° for a fully orthogonal nonplanar amide bond. Both χ_N and χ_C describe the tetrahedral character on the nitrogen and carbon, respectively, and range from 0° for a fully planar amide to 60° for fully pyramidalized amide bonds. In 2015, Szostak identified the additive Winkler–Dunitz distortion parameter $(\tau + \chi_N)$ as a means to more accurately predict structural and energetic properties [12]. The additive parameter is an extremely powerful tool for predicting the properties of distorted amides, corresponding linearly to N–C(O) bond length, *N*- vs. *O*-protonation affinity, infrared frequencies, resonance energies, atomic charges, and frontier molecular orbital energies [12]. Nearly the entire Winkler–Dunitz scale is represented by Type II bridged lactams prepared via synthetic efforts [5, 8]. Type I bridged lactams tend to be more flexible and thus do not span the entire range of the Winkler–Dunitz scale, limiting their usefulness in comprehensive understanding of distorted amides (Figure 1.3).

It should be noted that χ_C values for bridged lactams are generally close to 0° (even for relatively undistorted bridged lactams) due to the heightened contribution of amino-ketone resonance form **1** (Scheme 1.1, *vide supra*). At this stage, it is important to note polarized resonance contributor **3** [13], which corresponds to a nitrogen-to-carbon π-electron transfer with little oxygen resonance overlap. Polarized resonance contributor **3** describes the considerably larger N–C(O) bond lengthening compared with a considerably smaller C=O bond lengthening observed upon amide bond distortion [1, 14, 15]. According to the Wiberg–Bader theory of atoms in molecules (AIM), amide resonance stabilization is attributed to the hybridization change of nitrogen from sp^3 to sp^2 in planarizing an orthogonal amide bond. The validity of this polarized resonance model **3** has been a topic of considerable ongoing debate, with recent extensive computational modeling of Type II bridged lactam amide bond rotation demonstrating structural and energetic changes consistent with classical resonance form **1** [12].

An important and underappreciated aspect of amidic distortion is the bending of the amide carbonyl oxygen toward nitrogen. Notably, C=O bending is indicative of impending N–C(O) bond cleavage [16, 17]. In 2016, Stoltz and coworkers proposed the bending angle parameter ξ to describe the deviation from the imaginary CCN angle bisector (Figure 1.4) [16]. The ξ value is calculated by the equation shown in Figure 1.4, with a positive ξ corresponding to bending toward nitrogen and a negative ξ corresponding to bending toward carbon. The amide carbonyl bending effect was first discussed by Bürgi and Schmidt in 1985 in the context of crystallographic and molecular orbital calculations of lactones and lactams [17]. In these studies, an anomeric effect was proposed to reduce a destabilizing mixing of an oxygen *p*-type

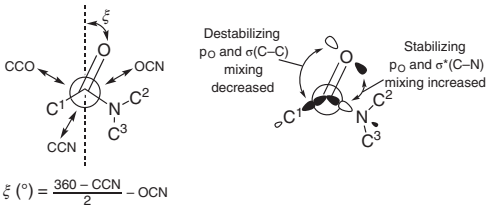

Figure 1.4 Definition of Bürgi C=O bending parameter ξ proposed by Stoltz and MO proposal for stabilizing effect of C=O bending.

lone pair orbital with the C–C(O) bonding orbital with simultaneous stabilizing mixing of the oxygen *p*-type orbital with the C–N antibonding orbital. Reported values of ξ deviate significantly from computational models [12, 16, 17]; therefore only ξ values derived from X-ray crystal structures will be discussed. Bridged lactam crystal structures published prior to the formalization of the ξ parameter will be presented with ξ values determined from crystal structures available via the Cambridge Crystallographic Data Centre when possible, thus some of the values shown here are not reported in the primary literature.

In addition to the Bürgi–Winkler–Dunitz parameters, amidic distortion has been quantified by the sum of three bond angles at nitrogen, θ, and the hinge angle of the carbonyl carbon with respect to the plane defined by the nitrogen atom and its two substituents, α (Figure 1.5) [18]. For an idealized sp^2-hybridized nitrogen atom $\theta = 360°$ and $\alpha = 180°$, whereas for a sp^3-hybridized nitrogen atom $\theta = 328.4°$ and $\alpha = 125°$.

1.2.2 Bond Lengths, Bond Angles, and Spectroscopic Properties of Bridged Lactams

Throughout the later sections of this chapter, examples of bridged lactams will be presented with their respective Winkler–Dunitz parameters and other relevant spectroscopic properties. Kirby's twisted amide (**8**) is presented in the following text in comparison to computationally predicted values for *N*-methyl-2-piperidone (**9**) as an instructive example of the amino-ketone nature of bridged lactams engendering electrophilicity akin to an acid chloride (Figure 1.6) [15, 19]. Kirby's amide (**8**) contains a nearly perpendicular amide bond ($\tau = 90.5°$) with a 0.150 Å longer N–C(O) bond but only a 0.037 Å longer N–C(O) bond when compared with lactam **9**.The θ value of 325.7° indicates that the nitrogen atom is sp^3 hybridized compared to the nearly ideal sp^2 hybridization of lactam **9** ($\theta = 358.9°$). Notably, the θ value of 325.7° is identical to the sum of bond angles at nitrogen in 1,4-diazabicyclo[2.2.2]octane (DABCO) and reminiscent of a typical θ value for trialkylamines [20]. In addition to these physical parameters, both the ^{13}C NMR and IR spectroscopic values are indicative of a aldehyde-like C=O bond in Kirby's amide **8**, whereas **9** displays spectroscopic properties typical of a lactam C=O bond [21]. The aldehydic nature of the

Figure 1.5 Definition of amide angle parameters θ and α.

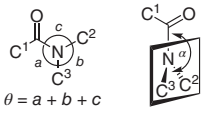

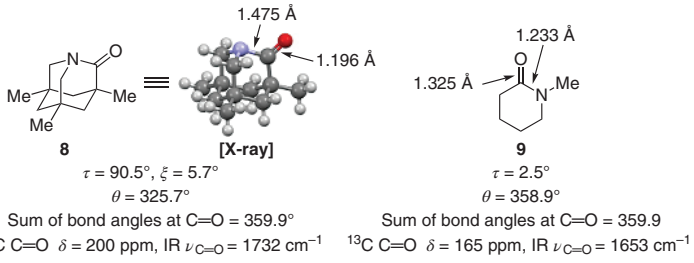

8 [X-ray]
$\tau = 90.5°$, $\xi = 5.7°$
$\theta = 325.7°$
Sum of bond angles at C=O = 359.9°
^{13}C C=O $\delta = 200$ ppm, IR $\nu_{C=O} = 1732$ cm^{-1}

9
$\tau = 2.5°$
$\theta = 358.9°$
Sum of bond angles at C=O = 359.9
^{13}C C=O $\delta = 165$ ppm, IR $\nu_{C=O} = 1653$ cm^{-1}

Figure 1.6 Comparison of Kirby's amide **8** and *N*-methyl-2-piperidone (**9**).

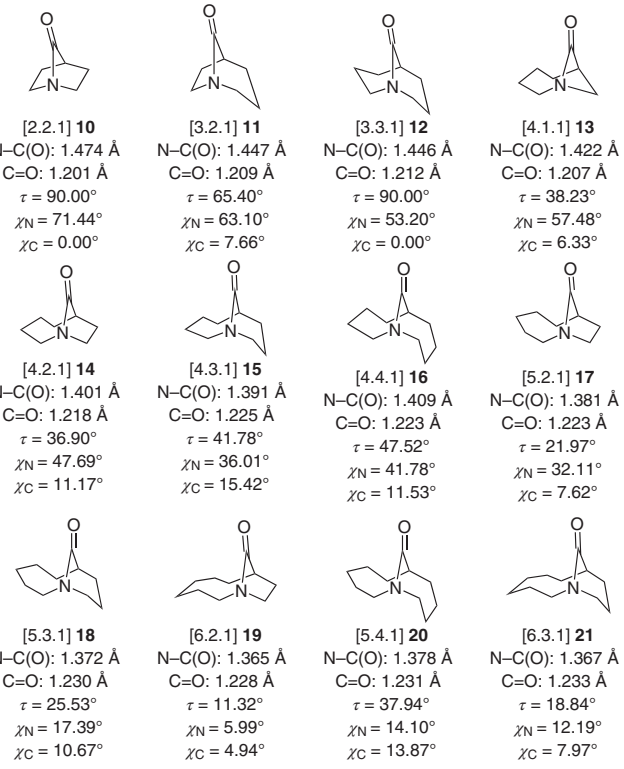

[2.2.1] **10**
N–C(O): 1.474 Å
C=O: 1.201 Å
$\tau = 90.00°$
$\chi_N = 71.44°$
$\chi_C = 0.00°$

[3.2.1] **11**
N–C(O): 1.447 Å
C=O: 1.209 Å
$\tau = 65.40°$
$\chi_N = 63.10°$
$\chi_C = 7.66°$

[3.3.1] **12**
N–C(O): 1.446 Å
C=O: 1.212 Å
$\tau = 90.00°$
$\chi_N = 53.20°$
$\chi_C = 0.00°$

[4.1.1] **13**
N–C(O): 1.422 Å
C=O: 1.207 Å
$\tau = 38.23°$
$\chi_N = 57.48°$
$\chi_C = 6.33°$

[4.2.1] **14**
N–C(O): 1.401 Å
C=O: 1.218 Å
$\tau = 36.90°$
$\chi_N = 47.69°$
$\chi_C = 11.17°$

[4.3.1] **15**
N–C(O): 1.391 Å
C=O: 1.225 Å
$\tau = 41.78°$
$\chi_N = 36.01°$
$\chi_C = 15.42°$

[4.4.1] **16**
N–C(O): 1.409 Å
C=O: 1.223 Å
$\tau = 47.52°$
$\chi_N = 41.78°$
$\chi_C = 11.53°$

[5.2.1] **17**
N–C(O): 1.381 Å
C=O: 1.223 Å
$\tau = 21.97°$
$\chi_N = 32.11°$
$\chi_C = 7.62°$

[5.3.1] **18**
N–C(O): 1.372 Å
C=O: 1.230 Å
$\tau = 25.53°$
$\chi_N = 17.39°$
$\chi_C = 10.67°$

[6.2.1] **19**
N–C(O): 1.365 Å
C=O: 1.228 Å
$\tau = 11.32°$
$\chi_N = 5.99°$
$\chi_C = 4.94°$

[5.4.1] **20**
N–C(O): 1.378 Å
C=O: 1.231 Å
$\tau = 37.94°$
$\chi_N = 14.10°$
$\chi_C = 13.87°$

[6.3.1] **21**
N–C(O): 1.367 Å
C=O: 1.233 Å
$\tau = 18.84°$
$\chi_N = 12.19°$
$\chi_C = 7.97°$

Figure 1.7 Geometric parameters for optimized structures of Type II bridged lactams calculated at the MP2/6-311++G(d,p) level. Source: Modified from Szostak et al. [12b].

N–C(O) bond is further characterized by the loss of CO from Kirby's amide upon electron-impact ionization.

Szostak utilized *ab initio* molecular orbital calculations to study the relationships between the structures of synthetically accessible Type II bridged lactams spanning the Winkler–Dunitz scale and their properties (Figure 1.7) [12]. In this series, increasing additive parameter ($\tau + \chi_N$) had excellent linear correlation with increasing N–C(O) bond length (Chart 1.1). Importantly, plotting of τ vs. N–C(O) bond length or χ_N vs. N–C(O) bond length resulted in more scattered correlations

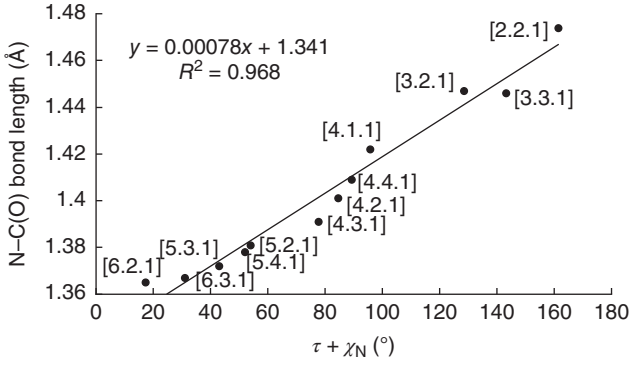

Chart 1.1 Plot of N–C(O) bond length vs. additive parameter for Type II bridged lactams in Figure 1.7. Source: Modified from Szostak et al. [12b].

(R^2 = 0.87 and 0.88, respectively, not shown). While the N–C(O) bond increased in length with increasing distortion, the C=O bond length did not appreciably change, consistent with amino-ketone resonance (**1** and **2**, Figure 1.1). This model should serve as a predictive tool of amide bond N–C(O) length upon distortion from planarity.

1.2.3 *N*- vs. *O*-protonation and Methylation and Structural Effects of *N*-coordination

A planarized amide bond favors *O*-protonation by approximately 10–15 kcal/mol (Scheme 1.2) [1]. The resulting *O*-protonated amide **22** benefits from approx. 40 kcal/mol of resonance stabilization [22] with resonance forms **22** and **23**, whereas *N*-protonated amide **24** cannot benefit from this resonance stabilization [9c]. Notably, *O*-protonation results in significant shortening of the N–C(O) with increased double bond character. In planarized amide bonds, the nitrogen lone pair contributes significantly to the HOMO of the amide system with its contribution denoted as π_N [1, 23]. As the amide bond is distorted from planarity and the nitrogen becomes pyramidalized, the lone pair contribution to the HOMO shifts toward lone pair character (n_N), resulting in a shift in *N*/*O*-protonation

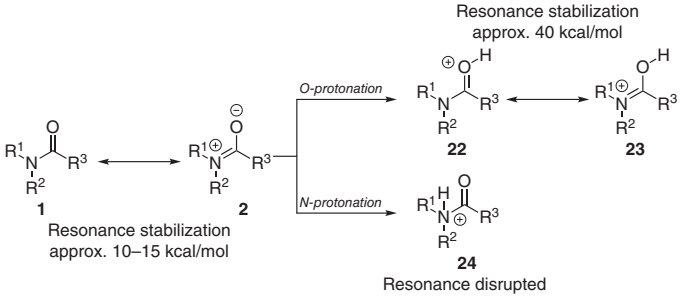

Scheme 1.2 *N*- vs. *O*-protonation of amides. Source: Greenberg et al. [1].

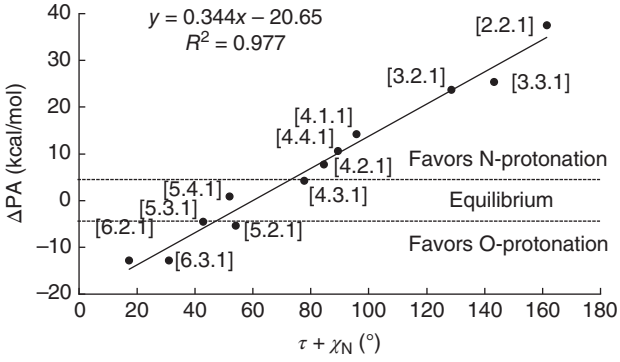

Chart 1.2 Plot of ΔPA (defined as $PA_N - PA_O$) for Type II bridged lactams in Figure 1.7.

aptitude [1, 24]. The *N*-protonation of amides is an important mode of reactivity for understanding processes such as σ C–N bond cleavage and *N*-acyl transfer reaction [25].

Before discussing specific examples of *N*- and *O*-protonation/methylation, it is informative to discuss the relationship between the additive Winkler–Dunitz parameter and *N*- vs. *O*-protonation affinity. In their 2015 studies, Szostak and coworkers found excellent linear correlation between the additive Winkler–Dunitz parameter and the difference in *N*- vs. *O*-proton affinity (PA), ΔPA, defined as $PA_N - PA_O$ for Type II bridged lactams shown in Figure 1.6 (*vide supra*) (Chart 1.2) [12]. This model divides the bridged lactams studied into three regimes: (i) lactams favoring *O*-protonation (ΔPA = −4.5 to −12.8 kcal/mol): [5.2.1], [5.3.1], [6.2.1], and [6.3.1], (ii) the [5.4.1] lactam that is expected to be in equilibrium between *O*- and *N*-protonation (ΔPA = 0.9 kcal/mol), and (iii) lactams favoring *N*-protonation (ΔPA = 4.3–37.5 kcal/mol): [2.2.1], [3.2.1], [3.3.1], [4.1.1], [4.2.1], and [4.3.1]. This provides a powerful method for prediction of the site of amide protonation and is in excellent agreement with examples comprehensive examinations of protonation affinity by Greenberg [22, 24, 26]. Notably, the *O*-protonation models of amides **14–21** had significantly longer C=O bonds than N–C(O) bonds, further supporting the classical amide resonance model (resonance contributors **1** and **2**). Szostak later modeled ΔPA in a series of Tröger's base twisted amides; however, these extremely twisted cases do not provide an ideal setting for studying *N*- vs. *O*-protonation [27].

The first experimental observations of *N*-protonation and *N*-methylation in bridged lactams were disclosed by Pracejus [28] and Yahkontov [29]. Here, some key examples of *N*- vs. *O*-protonation and methylation site selectivity are presented, along with relative parameters to demonstrate the relationship between amidic distortion and reactivity. Kirby's bridged lactam **8** undergoes quantitative *N*-methylation with excess Meerwein's salt as a desiccant to afford moisture-sensitive bridged lactam salt **25** [15b] (Scheme 1.3).

Treatment of lactam **8** with HCl did not allow isolation because of an inseparable hydrolysis by-product, thus characterization of the cation **26** was enabled treatment with anhydrous *p*-TsOH in $CDCl_3$. Spectroscopically, a significant shift of the

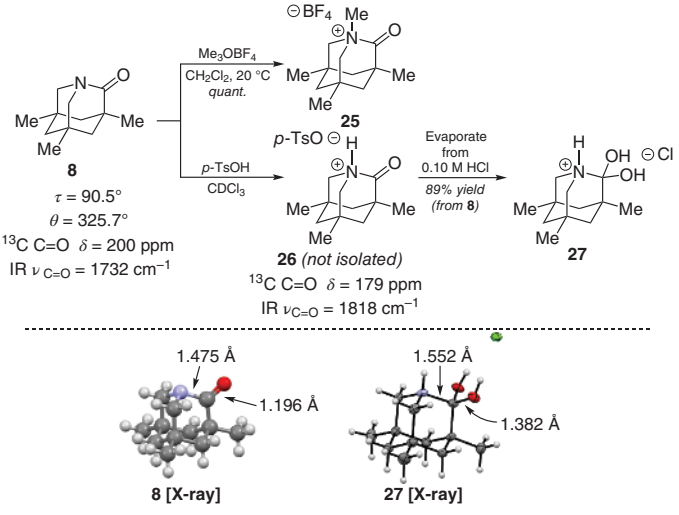

Scheme 1.3 *N*-methylation and *N*-protonation of Kirby's twisted amide **8**.

carbonyl ^{13}C signal from 200 to 179 ppm and IR signal frequency from 1732 to 1818 cm^{-1} was observed, although the IR frequency shift was extremely sensitive to trace moisture. Evaporation of tosylate salt **26** from 0.10 M HCl provided crystalline hydrate **27**. Notably, the 1.552 Å N–C bond is one of the longest N–C bonds recorded to date and the C–O(H) bonds are unusually short at 1.382 Å. This hydrate may be important for understanding intermediates in *N*-acyl transfer reactions in distorted amides [25].

Brown [30] demonstrated that [3.2.2] lactam **28** undergoes *N*-methylation selectively, whereas a more flexible (and therefore less distorted) [3.3.2] analog (**31**) is selectively methylated at oxygen (Scheme 1.4). Although specific parameters of

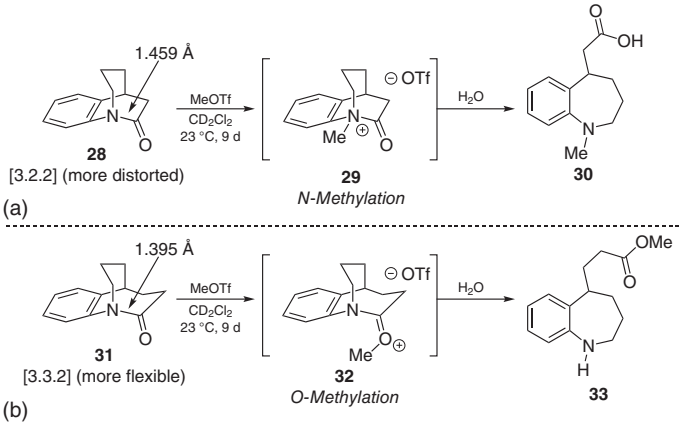

Scheme 1.4 *N*-methylation vs. *O*-methylation in [3.2.2] vs. [3.3.2] systems.

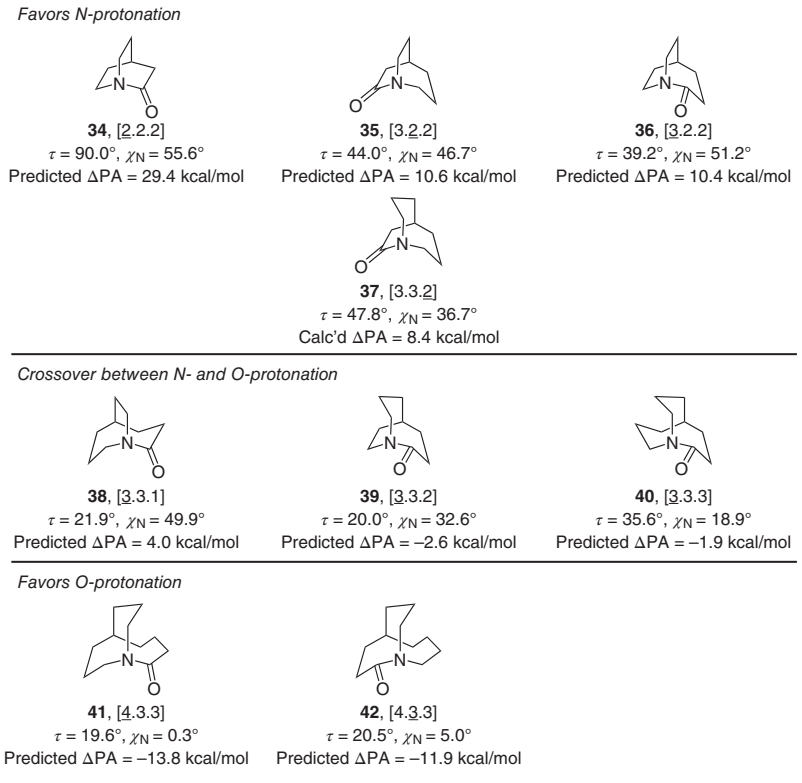

Figure 1.8 *Ab initio* MO calculated structures of Type I bridged lactams and distortion parameters by Greenberg with predicted ΔPA (defined as $PA_N - PA_O$) calculated using the trendline from Chart 1.2.

τ and χ_N are not directly reported, the calculated N–C(O) bond lengths of 1.459 and 1.395 Å for lactams **28** and **31**, respectively, demonstrate that **28** contains a much more distorted amide bond than **31**. It should be mentioned that Brown is careful to indicate that it is unclear if these reactions are the result of kinetic or thermodynamic selectivity. Greenberg later predicted *N*- vs. *O*-protonation with *ab initio* molecular orbital (MO) calculations for [2.2.2] to [4.3.3] bridged lactam scaffolds related to the Brown systems (Figure 1.8) [22, 26]. The "crossover" point between *N*- and *O*-site selection was found in [3.3.1], [3.3.2], and [3.3.3] systems. We present predicted ΔPA values in Figure 1.7 calculated using the trendline of Chart 1.2 [12] for this discussion, noting these values agree with Greenberg's predictions for *N*- vs. *O*-protonation selectivity.

Greenberg demonstrated an experimental example of crossover between *N*-protonation and *O*-protonation with [3.3.1] lactam **43** ($\tau = 19.8°$ and $\chi_N = 49.7°$) (Scheme 1.5) [31]. When lactam **43** is treated with H_2SO_4, a 4 : 1 ratio of *N*-protonation (**44**) and *O*-protonation (**45**) is measured at equilibrium. Amidic distortion is accompanied by a large degree of nitrogen pyramidalization, with significantly smaller pyramidalization of the carbonyl carbon (*vide supra*). On this basis, Greenberg proposed that the degree of distortion for complexation of other

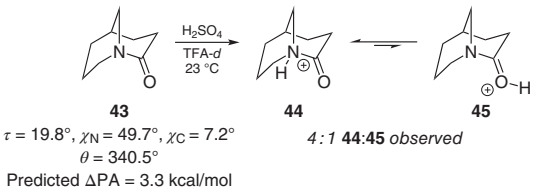

Scheme 1.5 *N*- and *O*-protonation crossover in a [3.3.1] lactam system. Source: Modified from Sliter et al. [31].

species should vary significantly. For example, complexation of "hard" Lewis acids such as Na^+ should intrinsically favor *O*-binding and thus significant distortion of the amide bond would be required to achieve preferential *N*-binding, whereas "soft" Lewis acids such as Cu^{2+} do not require a large degree of nitrogen pyramidalization for preferential *N*-binding [1, 31]. Importantly, amide bond *N*-binding of Cu^{2+} has been demonstrated as a mode for lowering the barrier to *cis*/*trans* peptidyl-prolyl isomerization in β-2-microglobulin [32].

In general, the *N*-coordination of amides causes significant distortion of the amide bond. Of the bridged lactams that have been synthesized to date, the *N*-coordinated bridged lactams have proven to be the most distorted and reactive of the series. The first direct crystallographic comparison between bridged lactams and their *N*-protonated form was reported by Aubé in 2010 (Scheme 1.6) [33]. *N*-protonation of lactam **46** with *p*-TsOH enabled isolation and crystallization of salt **47**, which displays extensive pyramidalization of the amide nitrogen compared with parent lactam **46**. The increase of χ_N from 31.6° to 52.1° demonstrates that nitrogen atom has significantly more sp^3 character ($\chi_N = 60°$ for an idealized sp^3 nitrogen atom). Comparison of the crystal structures of **46** and **47** also reveals a flattening ($\chi_C = 12.8°$ to $\chi_C = 1.4°$) and slight shortening of the C=O bond (1.218 to 1.192 Å), a significant twisting of the C–N bond ($\tau = 51.5°$ to $\tau = 81.9°$), and a large increase in C=O bending toward nitrogen ($\xi = 0.2°$ to $\xi = 5.1°$).

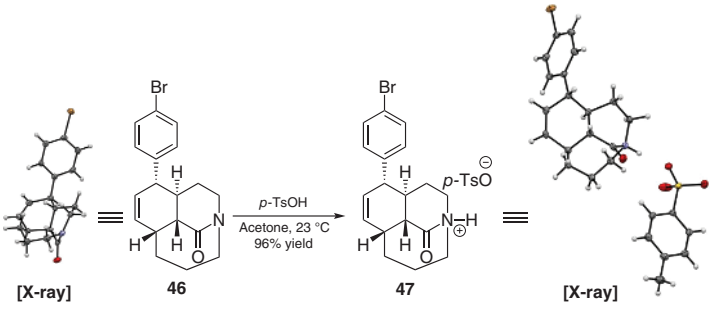

Amide	N–C(O) (Å)	C=O (Å)	χ_N (°)	χ_C (°)	τ (°)	ξ (°)
46	1.387	1.218	36.1	12.8	51.5	0.2
47	1.502	1.192	52.1	1.4	81.9	5.1

Scheme 1.6 First direct crystallographic comparison of a bridged lactam and its *N*-protonated form. Source: Modified from Szostak et al. [33].

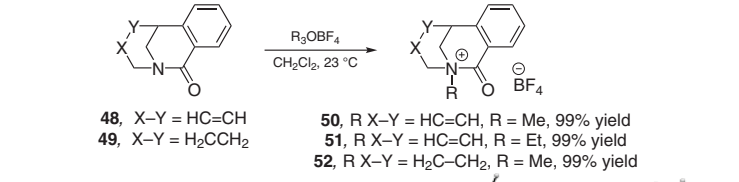

48, X–Y = HC=CH
49, X–Y = H_2CCH_2

50, R X–Y = HC=CH, R = Me, 99% yield
51, R X–Y = HC=CH, R = Et, 99% yield
52, R X–Y = H_2C–CH_2, R = Me, 99% yield

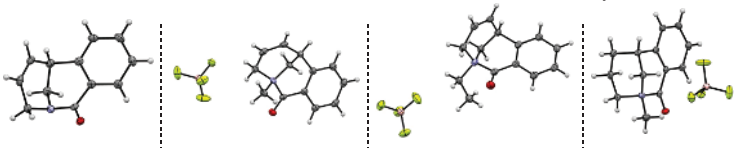

48 [X-ray] 50 [X-ray] 51 [X-ray] 52 [X-ray]

Amide	N–C(O) (Å)	C=O (Å)	χ_N (°)	χ_C (°)	τ (°)	ξ (°)
48	1.386	1.226	49.7	7.1	30.7	0.4
50	1.554	1.192	58.3	1.0	44.0	6.0
51	1.546	1.192	60.4	0.2	41.7	5.6
52	1.536	1.196	59.3	3.6	55.2	5.3

Scheme 1.7 Crystallographic comparison of a bridged lactam and *N*-alkylated bridged lactams. Source: Modified from Hu et al. [34].

Similarly, the first crystallographic structures of *N*-methylated bridged lactams and a parent bridged lactam were demonstrated in 2016 by Szostak (Scheme 1.7) [34]. As observed in the *N*-protonation of lactam **46**, *N*-alkylation of lactam **48** results in a dramatic lengthening and twisting of the N–C(O) bond, a slight shortening of the C=O bond, an increased pyramidalization of nitrogen, and a significant bending of the carbonyl toward nitrogen. Szostak also found that while lactam **48** protonates exclusively on nitrogen, *O*-coordination could be achieved nearly quantitatively via treatment with $AgSbF_6$, resulting in a rare example of an *O*-coordinated amide crystal structure (Scheme 1.8). Directly comparing the crystallographic data demonstrates the incredible structural impact of *N*- and *O*-coordination, with *O*-coordination reinforcing double bonding character of the N–C(O) bond. Interestingly, complex **53** is a rare example of a molecular wire where

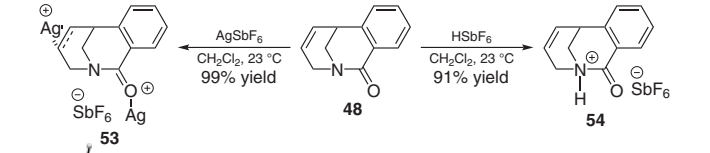

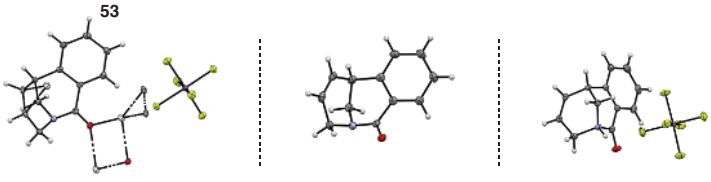

53 [X-ray] 48 [X-ray] 54 [X-ray]

Amide	N–C(O) (Å)	C=O (Å)	χ_N (°)	χ_C (°)	τ (°)	ξ (°)
48	1.386	1.226	49.7	7.1	30.7	0.4
53	1.355	1.262	47.7	5.8	33.3	1.9
54	1.539	1.196	55.0	0.7	42.0	6.9

Scheme 1.8 Divergent *N*- vs. *O*-coordination and crystallographic data.

each silver cation is coordinated to the olefin and an amide oxygen in an infinite chain structure [35].

N-coordination of bridged lactams has enabled isolation and characterization of some of the most twisted amides prepared to date with τ values c. 90°, indicating complete orthogonality of the amide bond. In closing this discussion, we highlight the structural features of some of these lactams and their parent lactams. It is important to note that in many cases, the parent lactams have not been successfully isolated and characterized, thus data presented is computationally derived. The reactivity of these systems will be further discussed in Section 1.3 (*vide infra*).

In 2006, Stoltz completed the synthesis of Type I [2.2.2] lactam **34·HBF$_4$**, which bears an extremely twisted amide bond (Scheme 1.9) [36, 37]. Isolation as the tetrafluoroborate salt via the Aubé–Schmidt reaction from azide **55** under rigorously anhydrous conditions was necessary to avoid nucleophilic attack from a more coordinating counter-anion [38]. Similarly, in 2016 Stoltz reported the synthesis of the [2.2.1] Type II bridged amides **10·HBF$_4$** and **10·BF$_3$**, utilizing the Aubé–Schmidt strategy [16]. Compound **10·HBF$_4$** was stable enough for rapid characterization by spectroscopic techniques, but readily decomposed to the more stable trifluoroborate **10·BF$_3$**, which provided X-ray quality crystals. The crystallographic data of **34·HBF$_4$** and **10·BF$_3$** reveal two of the most twisted amide bonds known to date. In both molecules, the amide bond achieves complete orthogonality, the nitrogen atoms are fully pyramidalized, and a large bend of the C=O bond toward

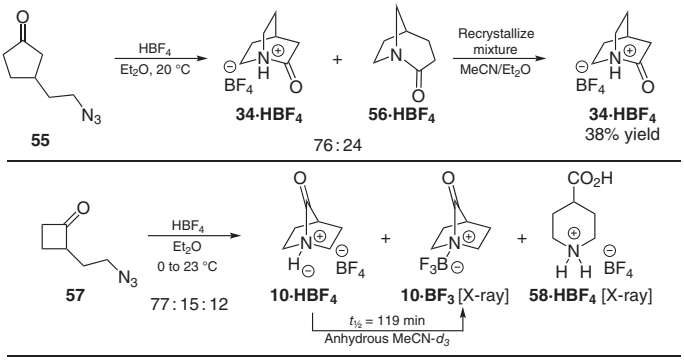

34·HBF$_4$ [X-ray] 10·BF$_3$ [X-ray]

Amide	N–C(O) (Å)	C=O (Å)	χ_N (°)	χ_C (°)	τ (°)	ξ (°)
34 [calculated]	1.504	1.167	57.6	0.0	89.9	—
34·BF$_4$ [X-ray]	1.526	1.192	59.5	0.2	90.9	5.8
10 [calculated]	1.474	1.201	71.4	0	90.0	—
10·BF$_3$ [X-ray]	1.526	1.186	69.8	0	90.0	5.8

Scheme 1.9 Synthesis of [2.2.2] and [2.2.1] *N*-coordinated bridged lactams via the Aubé–Schmidt reaction with computational and crystallographic structural data. Source: Adapted from Yakhontov et al. [36] and Tani et al. [37].

nitrogen of 5.8° is measured. Aside from Stoltz's *N*-coordinated lactams, Kirby's 1-adamantan-2-one-based bridged lactams are the only bridged lactams that have a fully orthogonal amide bond with an additive Winkler–Dunitz parameter exceeding 100° in their neutral form [5, 15, 19, 39].

1.2.4 Twisted Amide Basicity and pK_a Measurements

The preferential *N*-protonation of bridged lactams is concomitant with a substantial increase in amide basicity. Pracejus and Yakhontov measured the pK_a of the conjugate acids of methylated 2-quinuclidoniums **59**–**61** and **62**, respectively, which were sterically shielded from hydrolysis (Figure 1.9) [28b, 29a, c]. The *N*-protonated 2-quinuclidinones [**59**·**H**]$^+$–[**62**·**H**]$^+$ (pK_a = 5.33–6.37) are situated between *O*-protonated *N*,*N*-dimethylformamide ([**63**·**H**]$^+$, pK_a = 0.0) and quinuclidinium (**64**, pK_a = 10.65) on a pK_a scale, demonstrating their significantly enhanced basicity relative to planar amides. Kirby subsequently validated the Pracejus and Yakhontov measurements utilizing a stopped-flow indicator method [40] to estimate the pK_a value of 5.2 for lactam **8** [15b]. Few pK_a values have been reported for bridged lactams, ostensibly due to their lability in nucleophilic solvents.

Stoltz and Julian examined kinetic proton affinity of 2-quinuclidonium [**34**·**H**]$^+$ in the gas phase via competitive fragmentation of proton bound dimers relative to reference bases [41]. An experimental PA value of 964.2 kJ/mol was determined, well in agreement with the computationally predicted PA of 944.3 kJ/mol. In contrast, a typical amide has a much lower PA within the range of 880–900 kJ/mol [42]. 2-Quinuclidonium ([**34**·**H**]$^+$) is hydrolyzed instantaneously in water, and the reverse reaction through either the amino acid or acid chloride has not been achieved in solution phase; however, collisional excitation of hydrolyzed derivative **59** in the gas phase leads to formation of [**34**·**H**]$^+$ (Scheme 1.10) [37]. Stoltz and Julian also calculated a significantly higher PA of 982.0 kJ/mol for Yakhontov's more hydrolytically stable lactam **62**, demonstrating that bridged lactam nucleophilicity does not correlate with increased hydrolytic lability [41, 43].

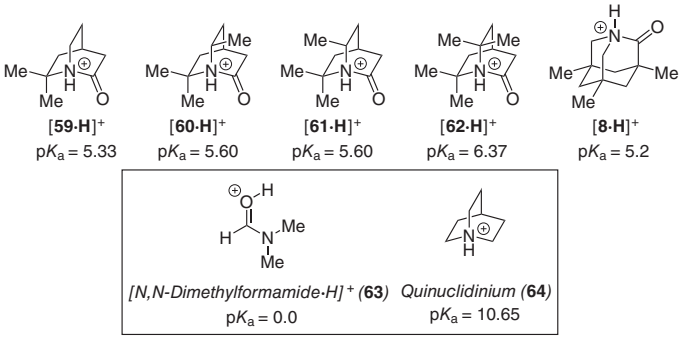

Figure 1.9 pK_a measurements (H_2O) of 2-quinuclidone derivatives [**59**·**H**]$^+$–[**62**·**H**]$^+$ and Kirby's lactam [**8**·**H**]$^+$.

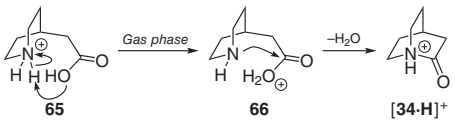

Scheme 1.10 Gas phase synthesis of 2-quiniclidone [**34**·**H**]$^+$. Source: Modified from Tani et al. [37].

1.3 Reactivity of Bridged Lactams

1.3.1 Reactivity of the Lactam Nitrogen

1.3.1.1 Hydrolysis of the N–C(O) Bond

The amide bond is well known for being recalcitrant toward hydrolysis, with half-lives ($t_{1/2}$) in neutral aqueous solution of hundreds of years [44]. Distortion of the amide linkage has a remarkable effect on this half-life [1], with some of the most strained bridged lactams undergoing instantaneous hydrolysis in water. Consequently, the increased sensitivity of bridged lactams often precludes the utilization of nucleophilic solvents (e.g. methanol, DMSO) in their synthesis and adds to the challenge of isolation and spectroscopic characterization of bridged lactams [4]. The study of bridged lactams hydrolysis has direct implications for the biological cleavage of peptide bonds that occur as a result of amidic distortion [1]. Here, we provide a general overview of bridged lactam hydrolysis in relation to amidic distortion. For a more comprehensive review, we direct the reader to a previously published reviews [4, 5]. Additionally, several theoretical studies have been performed to address the mechanism of hydrolysis in bridged lactams [45].

Early studies by Blackburn on the alkaline hydrolysis rate of strained *N*-aryl lactams demonstrated a dramatic rate increase correlated with increased twisting of the amide bond [46]. These studies demonstrated that distortion of the amide bond accelerates both the rate of nucleophilic attack at the amide carbonyl and the rate of nitrogen expulsion via collapse of the tetrahedral intermediate. Subsequently, Blackburn [47] and Brown [48] published a series of studies on the rate of hydrolysis of benzo-fused 2-quinuclidones (Scheme 1.11). The series of benzo-fused bridged lactams undergo hydrolysis in both acidic and basic water with rates several orders of magnitude larger compared with a planarized acetamide model (**73**). The best correlation between rate of hydrolysis and the structure of the bridged lactam is obtained when considering the additive Winkler–Dunitz parameter [12], which accounts for both amide bond twist and nitrogen pyramidalization.

Highly distorted amides typically undergo irreversible hydrolysis to the corresponding amino acid, [16, 39] with the notable exception of Kirby's 1-adamant-2-one **8** [15, 19]. While highly twisted bridged lactams provide insight into some of the more extreme cases of amide bond distortion, their lability preclude studies in nucleophilic solvents. In 2009, Aubé and coworkers demonstrated that medium-bridged lactams, while still significantly distorted (see Scheme 1.6 for distortion parameters), are thermodynamically and kinetically stable at acidic, neutral, and basic

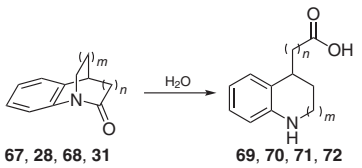

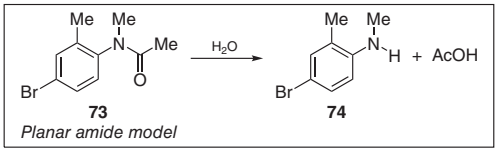

Amide	N–C(O) (Å)	C=O (Å)	χ_N (°)	χ_C (°)	τ (°)	ξ (°)	Base hydrolysis k_3 (M/s)	Acid hydrolysis k_3/K_3 (M/s)
67 ($n = m = 1$) [calculated]	—	—	63.4	0.0	90.0	—	2.6×10^{2}	2.3×10^{4}
28 $n = 1$, $m = 2$ [X-ray]	1.401	1.216	57.2	9.0	71.2	2.1	6.0×10^{1}	5.6×10^{1}
68 $n = 2$, $m = 1$ [X-ray]	1.413	1.225	52.8	11.0	75.6	2.4	1.7×10^{1}	3.0×10^{1}
31 $n = m = 2$ [X-ray]	1.370	1.233	38.6	4.3	34.4	0.0	5.1×10^{-4}	1.2×10^{-4}
73 [X-ray]	1.338	1.235	3.7	–1.5	1.3	0.4	2.2×10^{-5}	2.2×10^{-7}

Scheme 1.11 Rates of acidic and basic hydrolysis of benzo-fused 2-quinuclidones.

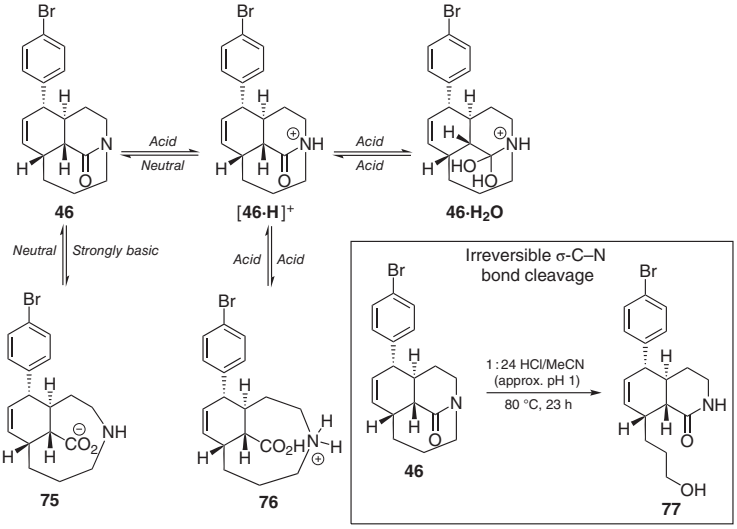

Scheme 1.12 pH-dependent speciation of medium-bridged lactam **46**. Source: Modified from Szostak et al [10].

pH in water (Scheme 1.12) [10]. Aubé and coworkers discovered that amide bond hydrolysis of amide **46** was reversible by performing a series of extraction and NMR experiments. Under basic conditions, the amide bond is hydrolyzed and conjugate base **75** is observed. In acid, speciation is observed between the *N*-protonated species $[\mathbf{46{\cdot}H}]^+$, hydrate $\mathbf{46{\cdot}H_2O}$, and the amide hydrolysis conjugate acid product **76**. Only after prolonged heating in pH 1 MeCN does medium-bridged lactam **46** undergo irreversible decomposition via σ-C–N bond cleavage. Importantly, these medium-bridged lactams represent an underexplored region of the

Winkler–Dunitz scale and could provide a potential avenue for study of the amide bond in nucleophilic solvents [49].

1.3.1.2 Cleavage of the σ C–N Bond

Cleavage of the σ C–N is a common pathway of reactivity for bridged lactams upon *N*-coordination. As discussed in Section 1.2.3, coordination of a bridged lactam nitrogen leads to increased bending of the C=O bond toward nitrogen, activating the σ C–N bond toward nucleophilic cleavage. The first examples of such reactivity were reported by Yakhontov; however, these examples were limited to tetramethyl-substituted 2-quinuclidone (**62**, Figure 1.9) for its ability to form tertiary carbocations [29a, c]. In efforts toward the total synthesis of stenine [50], Aubé observed hydrogenolysis of the σ C–N bond in a medium bridged lactam. A series of medium-bridged lactam analogs were subsequently investigated, demonstrating facile hydrogenolysis (with debromination) to lactam **78** [51], oxidative cleavage with DDQ to aldehyde **79**, and iodide cleavage of the σ C–N bond via *N*-methylation to iodide **80** (Scheme 1.13) [52]. Other examples demonstrated that the olefin was not required for the hydrogenolysis to proceed. Interestingly, utilization of deuterium gas in EtOD led to incorporation of a single deuterium atom on the propyl chain, implicating that cleavage may occur via direct insertion of Pd or displacement via a Pd hydride.

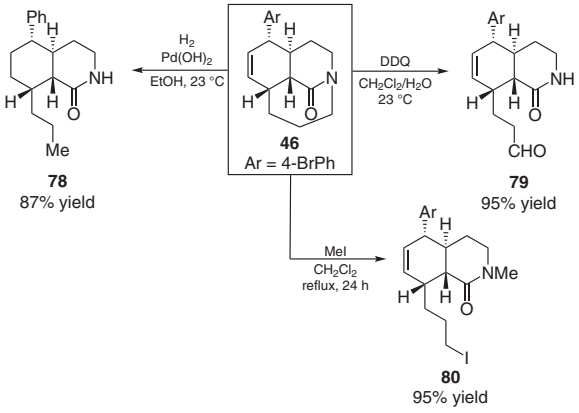

Scheme 1.13 σ C–N bond cleavage of a medium-bridged lactam. Source: Adapted from Lei et al. [52].

Szostak reported a "sew-and-cut" strategy for the two-step functionalization of isoquinoline-2-one ring systems (Scheme 1.14) [53]. Intramolecular Pd-catalyzed Heck reaction of aryl iodides **81a–s** generated bridged lactams with an additive Winkler–Dunitz parameter, $\tau + \chi_N$, in the range of 50°–60°. Cleavage of the σ C–N was then affected by a range of alkyl halides affording *N*-alkylated isoquinolin-2-ones **83a–s** in generally excellent yield. Control experiments suggest that the activation of the amide bond via *N*-alkylation is rate limiting. Interestingly, the lactams Szostak studied are more pyramidalized than twisted, possibly

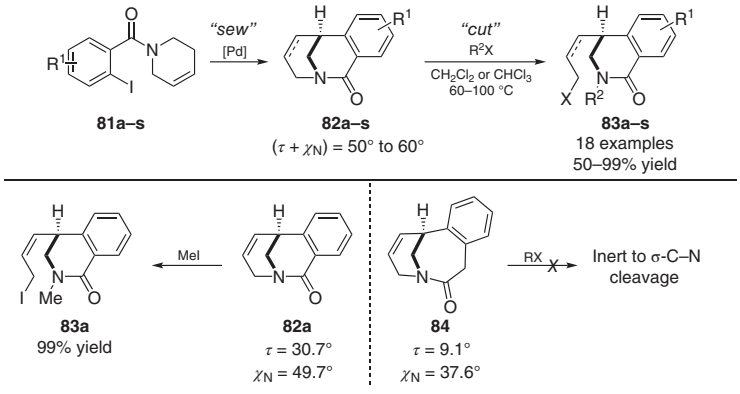

Scheme 1.14 "Sew-and-cut" approach to isoquinoline-2-one ring systems. Source: Adapted from Hu et al. [53].

indicating that the pyramidalization of the amide bond is more activating toward σ C–N bond cleavage. Ring-expanded bridged lactam **84** with a less distorted amide bond ($\tau + \chi_N = 46.7°$) was inert to cleavage of the σ C–N bond with alkyl halides.

1.3.2 Reactivity of the Carbonyl Group

The heightened electrophilicity of the twisted amide carbonyl coupled with the higher *O*-basicity of planarized amides allows an opportunity for divergent chemoselectivity in complex systems [4, 5]. Steric restriction of the amide bond in bridged lactams often enables isolation of stable tetrahedral intermediates resulting from 1,2-addition to the carbonyl [25]. A comprehensive review of reactions of the lactam carbonyl is not possible here; instead we provide a broad overview of general reactivity to highlight the amino-ketone resonance contribution in bridged lactams.

1.3.2.1 Heteroatom Nucleophiles

Yakhontov reported first nucleophilic cleavage of bridged lactam amide bonds with tetramethyl 2-quinuclidinone **62** with nucleophiles including alcohols, amines, hydrazines, and hydroxylamines (Scheme 1.15) [29a, c]. This reactivity is quite general for bridged lactam carbonyls despite the steric shielding in the present example (**62**) [4, 5]. In 2019, Szostak compared and modeled the reactivity of

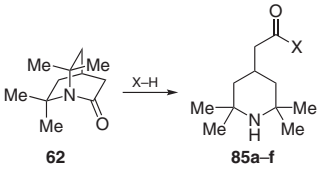

Entry	X–H	Conditions	Yield (%)
1	H_2O	Reflux, 30 min	94
2	MeOH	Reflux, 5 h	96
3	Morpholine	Reflux, 12 h	97
4	NH_2OH	EtOH, reflux, 2 h	62
5	NH_2NH_2	Xylenes, reflux, Dean–Stark, 5 h	63
6	NH_2NHPh	Xylenes, reflux, Dean–Stark, 12 h	64

Scheme 1.15 Bridged lactam bond cleavage with heteroatom nucleophiles. Source: Adapted from Levkoeva et al. [29a, c].

bridgehead lactam **82** against less reactive acyclic 3° anilides in intermolecular transamination with non-nucleophilic amines (not shown) [54, 55]. The reactivity of bridgehead lactams toward heteroatom nucleophiles has also been exploited in polymerization processes by Hall [56].

Condensation reactions with heteroatom nucleophiles including diols [15b], hydrazines [15b, 57], and amines [15b] are generally limited to adamantane or medium-bridged lactams as the scaffolding effects of these systems are required for product stability [4]. Ma and coworkers reported an elegant total synthesis of indole alkaloid communesin F wherein a bridged lactam facilitated the rapid synthesis of the assembly of the natural product core via a one-pot Staudinger/intramolecular condensation sequence (Scheme 1.16) [58].

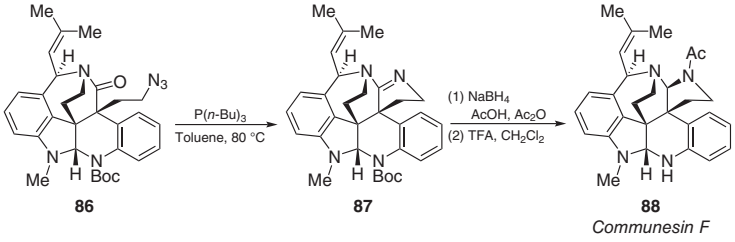

Scheme 1.16 Staudinger/intramolecular condensation in the total synthesis of communesin F by Ma. Source: Adapted from Zuo et al. [58].

1.3.2.2 Organometallics

Aubé reported the formation of ketones upon treatment of medium-sized bridged lactam **89** with an excess of organometallic reagents (Scheme 1.17, top) [57]. Despite addition of excess nucleophile, no addition to the ketone was observed. When tricyclic bridged lactams were treated with organolithium reagents, both the hemiaminal **92** and ketone **93** could be observed (Scheme 1.17, bottom). The steric bulk

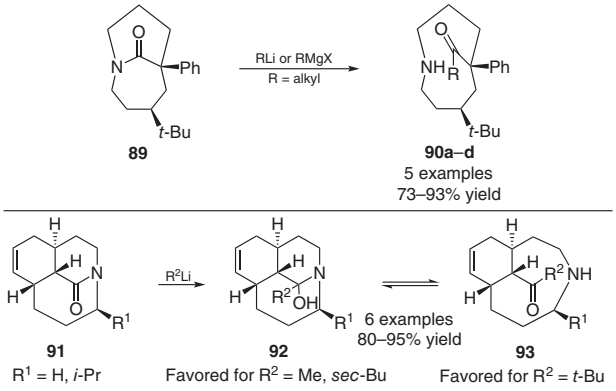

Scheme 1.17 Organometallic addition to medium-bridged lactams. Source: Adapted from Szostak et al. [57].

of the R^2 group determined the major product in the equilibrium, with hemiaminal **92** favored for R^2 = Me and *sec*-Bu and amino-ketone favored **93** for R^2 = *t*-Bu.

1.3.2.3 Reduction of the Carbonyl

While amides are typically inert to reduction by sodium borohydride, the ketone-like nature of the carbonyl in bridged lactams enables reactivity. Subsequent to the first reports of adamantane-based bridged lactam reduction by borohydride from Denzer and Ott [59] and Kirby [15b], Aubé demonstrated that moderately distorted bridged lactams **94** and **46** can be reduced (Scheme 1.18) [57]. Placement of an electron-withdrawing group α such as SO_2Me (**96**) to the bridgehead lactam results in an interesting C–C bond scission leading to formamide **98** in excellent yield. The stability of the hemiaminal products **95** and **99** are likely due to poor overlap between the nitrogen lone pair and the σ*(C–O).

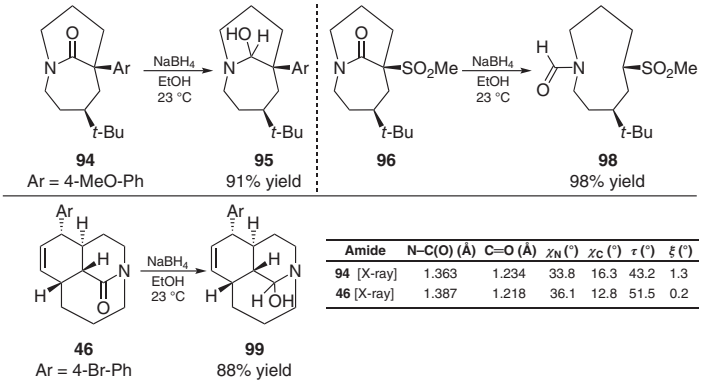

Amide	N–C(O) (Å)	C=O (Å)	χ_N (°)	χ_C (°)	τ (°)	ξ (°)
94 [X-ray]	1.363	1.234	33.8	16.3	43.2	1.3
46 [X-ray]	1.387	1.218	36.1	12.8	51.5	0.2

Scheme 1.18 Sodium borohydride reduction of bridged lactams.

In general, the more flexible a bridged lactam system is the more facile the full reduction of the amide bond is. This is best highlighted by examination of Thomas' efforts toward the total synthesis of stemofoline wherein reduction of rigid tropanone **100** with $LiAlH_4$ does not proceed past hemiaminal **101**. A subsequent transformation of the hemiaminal to the corresponding amino chloride is required for full reduction to amine **102** (Scheme 1.19, top) [60]. In contrast, Dolby achieved full reduction of the amide functionality in the highly flexible lactam **103** with a [6.6.2] ring system, which is more similar to a planarized amide (*vide supra*) [61].

1.3.2.4 Olefination and Epoxidation Reactions

The amino-ketone behavior of bridged lactams has also been demonstrated by their reactivity toward olefination and epoxidation conditions. In planar amides, olefination is typically impeded by the delocalization of nitrogen lone pair into the π*(CO) orbital, decreasing the sp^2 characteristic of the bond, thus rendering the planar amide bond inactive toward olefination. Epoxidation is similarly disrupted by resonance, and ring-opened products are obtained rather than epoxides. However, both types of reactions may be illustrated with sufficiently twisted

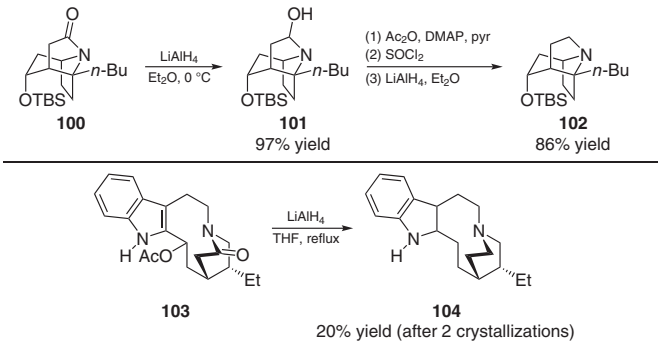

Scheme 1.19 Comparison of rigid and flexible bridged lactam reduction. Source: Adapted from Beddoes et al. [60a].

amide bonds as demonstrated by the examples in the following text from Aubé (Scheme 1.20) [57, 62]. Petasis olefination of bicyclic bridged lactam **89** generated olefin **105**, while Corey–Chaykovsky epoxidation formed stable amino epoxide **106**. Corey–Chaykovsky epoxidation was also effective in tricyclic bridged lactams such as **46**. Wittig olefinations are also effective in bridged lactam systems as first demonstrated by Kirby [15b].

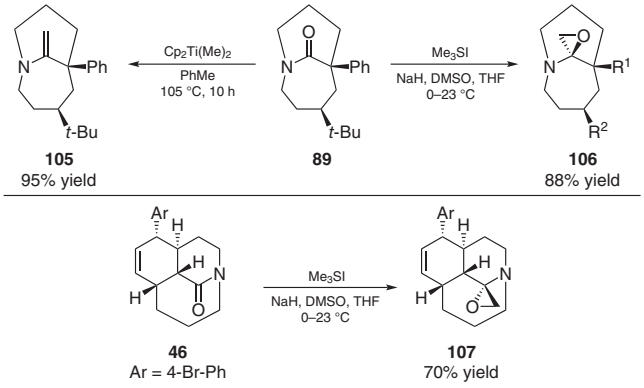

Scheme 1.20 Olefination and epoxidation of bridged lactams. Source: Adapted from Szostak et al. [57, 62].

1.3.2.5 Enolate and Conjugate Addition Chemistry

In limited examples, flexible bridged lactams have been utilized as nucleophiles in enolate functionalization [63] and in Friedel–Crafts reactions in indole-fused systems [64]. In [6.3.1] bridged lactam **108**, Ban demonstrated that several electrophiles could be utilized to accomplish C-alkylation and C-acylation (Scheme 1.21). With methyl iodoacetate and methyl bromoacetate, moderate yields of α-halogenation products **109c** and **109d** were obtained. In addition to α-functionalization of bridged lactams, Judd and coworkers demonstrated Rh-catalyzed conjugate addition of an aryl boronic acid with α,β-unsaturated bridged lactam **110** (Scheme 1.22) [65].

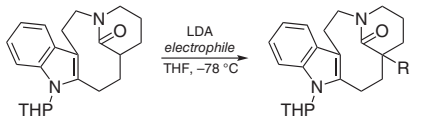

108 109a–g

Entry	Electrophile	Product	R	Yield (%)
1	Et–I	**109a**	Et	84
2	Allyl bromide	**109b**	Allyl	71
3	I–CH_2CO_2Me	**109c**	I	42
4	Br–CH_2CO_2Me	**109d**	Br	34
5	Cl–CH_2CO_2Me	**109e**	$C(O)CH_2Cl$	66
6	Ac_2O	**109f**	CO_2Me	90
7	$CH_2C(SOMe)(SMe)$	**109g**	$CH_2CH(SOMe)(SMe)$	71

Scheme 1.21 Enolate reactivity of [6.3.1] lactam **108**.

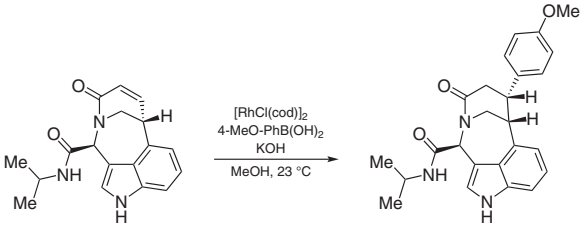

110 111
87% yield, >98 : 2 dr

Scheme 1.22 Rh-catalyzed conjugate addition with bridged lactam **110**. Source: Adapted from Ribelin et al. [65].

1.3.3 Polymerization Reactions

The strain of bridged lactams has been harnessed to drive polymerization reactions [56]. Inspired by reports from Stoltz [37] that the twisted amide 2-quinuclidone (**34**) formed polymeric material in attempts to neutralize the compound Gutekunst designed the first living polymerization of twisted amides with simple primary alkyl iodides employed as initiators (Scheme 1.23) [66]. Bridged lactam monomer

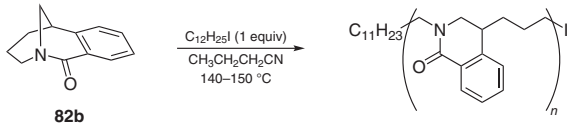

82b 112

Entry	Target DP (*n*)	Temp (°C)	Time (h)	Conversion (%)	$M_{n,theo}$ (kg/mol)	$M_{n,SEC}$ (kg/mol)	$Đ$
1	10	140	12	98	2.1	2.1	1.21
2	25	140	24	96	4.8	5.1	1.20
3	50	140	30	94	9.4	9.4	1.20
4	75	140	48	94	13.5	12.1	1.26
5	100	150	52	>95	18.1	17.3	1.26
6	200	150	64	91	34.4	24.3	1.46

Scheme 1.23 Halide-rebound polymerization of twisted amide **82b**. Source: Adapted from Fu et al. [66].

82b was observed to form polymers of linearly increasing molecular weights via halide-rebound polymerization. Gutekunst also reported the living ring-opening metathesis polymerization (ROMP) of an unsaturated bridged lactam with Grubbs III (Scheme 1.24) [67]. The calculated strain energy of 11.3 kcal/mol served as the primary driving force toward ROMP. Upon ring-opening, the amide could reintegrate into the conjugated planar system, promoting propagation of the polymer. To understand the role of amide distortion in the polymerization, another ROMP experiment was performed with a methine carbon in the place of the bridgehead nitrogen, which resulted in no conversion.

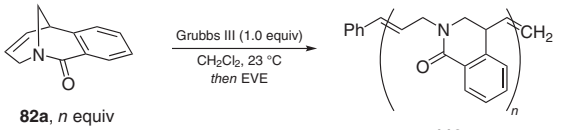

82a, *n* equiv

113

Entry	Target DP (*n*)	Time (h)	Conversion (%)	$M_{n,theo}$ (kg/mol)	$M_{n,SEC}$ (kg/mol)	$Đ$
1	10	2	95	1.9	1.9	1.21
2	25	2	93	4.4	4.6	1.20
3	50	2	91	8.6	9.0	1.20
4	100	2	91	16.9	15.2	1.20
5	200	2	89	27.6	33.1	1.26
6	500	3	91	84.7	63.4	1.46

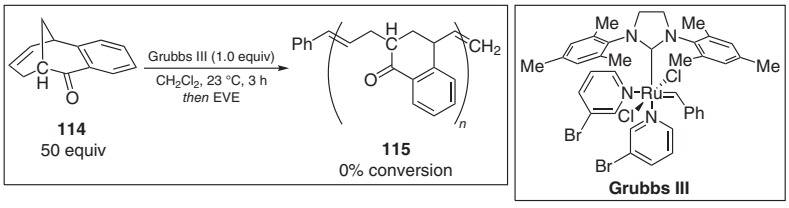

114
50 equiv

115
0% conversion

Grubbs III

Scheme 1.24 Living ROMP of unsaturated twisted amide **82a**. Source: Modified from Xu et al. [67].

1.3.4 Miscellaneous Reactions

1.3.4.1 Ring Opening via Olefin Metathesis

Szostak reported the selective C=C bond cleavage of twisted lactam **82a** containing alkene moieties by ring-opening metathesis with Grubbs II catalyst without any products resulting from N–C(O) or σ N–C bond cleavage (Scheme 1.25) [68]. Cinnamyl, aliphatic, and electron-deficient olefins could be utilized to produce the ring-opened products **116** and **117** with moderate to excellent selectivity for ring-opened product **116**. Computational modeling predicts that the ring strain of the bridged lactam **82a** (14.2 kcal/mol) is significantly higher than that of analogous amine (0.8 kcal/mol), ketone (0.0 kcal/mol), and hydrocarbon (1.0 kcal/mol). The analogous planar anilide resulted in >95% recovery of the starting material, highlighting the essential role of amidic strain energy of in the ring-opening metathesis.

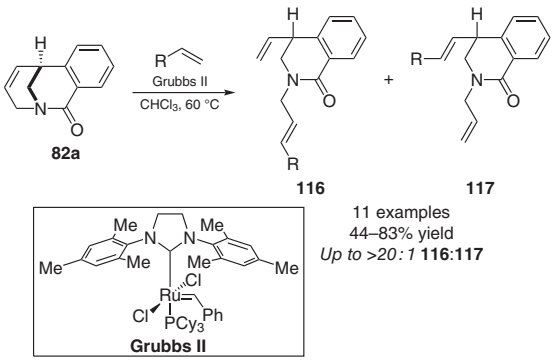

Scheme 1.25 Ring-opening metathesis of bridged lactam **82a**. Source: Adapted from Zhao et al. [68].

1.4 Conclusions and Outlook

Bridged lactams are the most successful models for studying the full range of amide bond distortion. The structure and reactivity of distorted amide bonds has wide-ranging applications, from amide bond rotation and cleavage in biological systems to applications in synthetic chemistry as reactive intermediates. The wealth of crystallographic and structural data now available provide valuable quantification of amide bond distortion with powerful predictive capabilities. While many valuable contributions to bridged lactam chemistry have been made since Lukeš first conceived of a bridged lactam in 1938 [3], there are many challenges that remain. First, no neutral bridged lactam with the exception of Kirby's adamantane-based bridged lactams has been prepared with an additive parameter $\tau + \chi_N$ exceeding 100° or 60% of maximum amide bond distortion [5]. Additionally, although nearly the entire Bürgi–Winkler–Dunitz scale is represented by bridged lactams synthesized to date, examples spanning the higher range of the distortion scale lack the structural diversity required for ample understanding of their stability [4, 5]. Finally, synthetic utilization of bridged lactams has mainly focused on hydrolysis and reactions akin to those of activated carbonyls. Given these limitations and the ubiquity of the amide bond, continued development of bridged lactams toward a comprehensive understanding of amide bond distortion will be invaluable.

References

1 Greenberg, A., Breneman, C.M., and Liebman, J.F. (ed.) (2000). *The Amide Linkage: Structural Significance in Chemistry, Biochemistry, and Materials Science*. New York: Wiley.

2 (a) Pauling, L. (1940). *The Nature of the Chemical Bond*. London: Oxford University Press. (b) Pauling, L. (1931). *J. Am. Chem. Soc.* 53: 1367–1400. (c) Liebman, J.F. and Greenberg, A. (2019). *Struct. Chem.* 30: 1631–1634.

3 Lukeš, R. (1938). *Collect. Czech. Chem. Commun.* 10: 148–152.

4 Szostak, M. and Aubé, J. (2013). *Chem. Rev.* 113: 5701–5765.

5 Szostak, R. and Szostak, M. (2019). *Molecules* 24: 274–290.

6 Yamada, S. (1999). *Rev. Heteroatom Chem.* 19: 203–236.

7 Liu, C. and Szostak, M. (2017). *Chem. Eur. J.* 23: 7157–7173.

8 Li, G., Ma, S., and Szostak, M. (2020). *Trends Chem.* 2: 914–928.

9 (a) Liu, J., Albers, M.W., Chen, C.M. et al. (1990). *Proc. Natl. Acad. Sci. U. S. A.* 87: 2304–2308. (b) Fisher, G. and Schmid, F.X. (1999). Peptidyl-prolyl cis/trans isomerases. In: *Molecular Chaperones and Folding Catalysts: Regulation, Cellular Functions and Mechanisms* (ed. B. Bakau). Boca Raton, FL: CRC Press. (c) Cox, C. and Lectka, T. (2000). *Acc. Chem. Res.* 33: 849–858. (d) Fisher, G. (2000). *Chem. Soc. Rev.* 29: 119–127.

10 Szostak, M., Yao, L., and Aubé, J. (2009). *J. Org. Chem.* 74: 1869–1875.

11 (a) Winkler, F.K. and Dunitz, J.D. (1971). *J. Mol. Biol.* 59: 169–182. (b) Dunitz, J.D. and Winkler, F.K. (1975). *Acta Crystallogr., Sect. B: Struct. Crystallogr. Cryst. Chem.* 31: 251–263.

12 (a) Szostak, R., Aubé, J., and Szostak, M. (2015). *Chem. Commun.* 51: 6395–6398. (b) Szostak, R., Aubé, J., and Szostak, M. (2015). *J. Org. Chem.* 80: 7905–7927.

13 (a) Wieberg, K.B. (1999). *Acc. Chem. Res.* 32: 922–929. (b) Wiberg, K.A. (2000). Origin of the amide rotational barrier. In: *The Amide Linkage: Structural Significance in Chemistry, Biochemistry, and Materials Science* (ed. A. Greenberg, C.M. Breneman and J.F. Liebman). New York: Wiley. (c) Kemnitz, C.R. and Loewen, M.J. (2007). *J. Am. Chem. Soc.* 129: 2521–2528.

14 Yamada, S. (1993). *Angew. Chem. Int. Ed.* 32: 1083–1085.

15 (a) Kirby, A.J., Komarov, I.V., Kowski, K., and Rademacher, P. (1999). *J. Chem. Soc., Perkin Trans.* 2: 1313–1316. (b) Kirby, A.J., Komarov, I.V., and Feeder, N. (2001). *J. Chem. Soc., Perkin Trans.* 2: 522–529.

16 Liniger, M., Vander Velde, D.G., Takase, M.K. et al. (2016). *J. Am. Chem. Soc.* 138: 969–974.

17 Nørskov-Lauritsen, L., Bürgi, H.-B., Hofmann, P., and Schmit, H.R. (1985). *Helv. Chim. Acta* 68: 76–82.

18 Otani, Y., Nagae, O., Naruse, Y. et al. (2003). *J. Am. Chem. Soc.* 125: 15191–15199.

19 (a) Kirby, A.J., Komarov, I.V., and Feeder, N. (1998). *J. Am. Chem. Soc.* 120: 7101–7102. (b) Kirby, A.J., Komarov, I.V., Wothers, P.D., and Feeder, N. (1998). *Angew. Chem. Int. Ed.* 37: 785–786.

20 Sorriso, S. (1982). *Chemistry of Functional Groups, Supplement F, Part 1* (ed. S. Patai), 1. Chichester: Wiley-Interscience.

21 Silverstein, R.M., Bassler, G.C., and Morrill, T.C. (1991). *Spectroscopic Identification of Organic Compounds*. New York: Wiley.

22 Greenberg, A. and Veranzi, C.A. (1993). *J. Am. Chem. Soc.* 115: 6951–6957.

23 (a) Treschanke, L. and Rademacher, P. (1985). *THEOCHEM* 122: 35–45. (b) Treschanke, L. and Rademacher, P. (1985). *THEOCHEM* 122: 47–56.

24 Morgan, J. and Greenberg, A. (2014). *J. Chem. Thermodyn.* 73: 206–212.

25 Adler, M., Alder, S., and Boche, G.J. (2005). *Phys. Org. Chem.* 18: 193–209.

26 Greenberg, A., Moore, D.T., and Dubois, T.D. (1996). *J. Am. Chem. Soc.* 118: 8658–8668.

27 Szostak, R. and Szostak, M. (2019). *J. Org. Chem.* 84: 1510–1516.

28 (a) Pracejus, H. (1959). *Chem. Ber.* 92: 988–998. (b) Pracejus, H., Kehlen, M., Kehlen, H., and Matschiner, H. (1965). *Tetrahedron* 21: 2257–2270. (c) Pracejus, H. (1965). *Chem. Ber.* 98: 2897–2905.

29 (a) Levkoeva, E.I., Nikitskaya, E.S., and Yakhontov, L.N. (1970). *Dokl. Akad. Nauk* 192: 342. (b) Kostyanovsky, R.G., Mikhlina, E.E., Levkoeva, E.I., and Yakhontov, L.N. (1970). *Org. Mass Spectrom.* 3: 1023–1029. (c) Levkoeva, E.I., Nikitskaya, E.S., and Yakhontov, L.N. (1971). *Khim. Geterotsikl. Soedin.* 378–384.

30 Werstiuk, N.H., Brown, R.S., and Wang, Q. (1996). *Can. J. Chem.* 74: 524–532.

31 Sliter, B., Morgan, J., and Greenberg, A. (2011). *J. Org. Chem.* 76: 2770–2781.

32 Eakin, C.M., Berman, A.J., and Miranker, A.D. (2006). *Nat. Struct. Mol. Biol.* 13: 202–208.

33 Szostak, M., Yao, L., Day, V.W. et al. (2010). *J. Am. Chem. Soc.* 132: 8836–8837.

34 Hu, F., Lalancette, R., and Szostak, M. (2016). *Angew. Chem. Int. Ed.* 55: 5062–5066.

35 Schwab, P.F.H., Levin, M.D., and Michl, J. (1999). *Chem. Rev.* 99: 1863–1934.

36 The original report of the synthesis of 2-quinuclidone reported by Yakhontov includes only nitrogen elemental analysis and has been called into question by Pracejus [30] and Stoltz [39]. For the original report by Yakhontov, see:Yakhontov, L.N. and Rubsitov, M.V. (1957). *J. Gen. Chem. USSR* 27: 83–87.

37 Tani, K. and Stoltz, B.M. (2006). *Nature* 441: 731–734.

38 Aubé, J. and Milligan, G.L. (1991). *J. Am. Chem. Soc.* 113: 8965–8966.

39 Komarov, I.V., Yanik, S., Ishchenko, A.Y. et al. (2015). *J. Am. Chem. Soc.* 137: 926–930.

40 Hine, J., Craig, J.C. Jr., Underwood, J.G. II, and Via, F.A. (1970). *J. Am. Chem. Soc.* 92: 5194–5199.

41 Ly, T., Krout, M., Pham, D.K. et al. (2007). *J. Am. Chem. Soc.* 129: 1864–1865.

42 Hunter, E.P. and Lias, S.G. (2005). Proton Affinity Evaluation. In: *NIST Chemistry Web Book*, NIST Standard Reference Database Number 69 (ed. P.J. Linstrom and W.G. Mallard), 20899. National Institute of Standards and Technology: Gaithersburg, MD.

43 Greenberg, A., Wu, G., Tsai, J.-C., and Chiu, Y.-Y. (1993). *Struct. Chem.* 4: 127–129.

44 (a) Radzicka, A. and Wolfenden, R. (1996). *J. Am. Chem. Soc.* 118: 6105–6109. (b) Smith, R.M. and Hansen, D.E. (1998). *J. Am. Chem. Soc.* 120: 8910–8913.

45 (a) Lopez, X., Mujika, J.I., Blackburn, G.M., and Karplus, M. (2003). *J. Phys. Chem.* 107: 2304–2315. (b) Mujika, J.I., Mercero, J.M., and Lopez, X. (2003). *J. Phys. Chem. A* 31: 6099–6107. (c) Mujika, J.I., Mercero, J.M., and Lopez, X. (2005). *J. Am. Chem. Soc.* 127: 4445–4453. (d) Mujika, J.I., Formoso, E., Mercero, J.M., and Lopez, X. (2006). *J. Phys. Chem. B* 110: 15000–15011. (e) Wang, B. and Cao, Z. (2011). *Chem. Eur. J.* 17: 11919–11929.

46 Blackburn, G.M. and Plackett, J.D. (1972). *J. Chem. Soc., Perkin Trans.* 2: 1366–1371.

47 Blackburn, G.M., Skaife, C.J., and Kay, I.T. (1980). *J. Chem. Res., Synop* . 294–295.

48 (a) Somayaji, V. and Brown, R.S. (1986). *J. Org. Chem.* 51: 2676–2686. (b) Wang, Q.P., Bennet, A.J., Brown, R.S., and Santarsiero, B.D. (1990). *Can. J. Chem.* 68: 1732–1739. (c) Bennet, A.J., Wang, Q.-P., Slebocka-Tilk, H. et al. (1990). *J. Am. Chem. Soc.* 112: 6383–6385. (d) Wang, Q.P., Bennet, A.J., Brown, R.S., and Santarsiero, B.D. (1991). *J. Am. Chem. Soc.* 113: 5757–5765.

49 Szostak, M. and Aubé, J. (2011). *Org. Biomol. Chem.* 9: 27–35.

50 Golden, J.E. and Aubé, J. (2002). *Angew. Chem. Int. Ed.* 41: 4316–4318.

51 For additional examples of hydrogenolysis of σ C–N bonds, see:Szostak, M. and Aubé, J. (2009). *Org. Lett.* 11: 3878–3881.

52 Lei, Y., Wrobleski, A.D., Golden, J.E. et al. (2005). *J. Am. Chem. Soc.* 127: 4552–4553.

53 Hu, F., Nareddy, P., Lalancette, R. et al. (2017). *Org. Lett.* 19: 2386–2389.

54 Li, G., Ji, C.-L., Hong, X., and Szostak, M. (2019). *J. Am. Chem. Soc.* 141: 11161–11172.

55 For a recent review on transamidation reactions, see:Li, G. and Szostak, M. (2020). *Synthesis* 52: 2579–2599.

56 Hall, H.K. Jr., and El-Shekeil, A. (1983). *Chem. Rev.* 83: 549–555.

57 Szostak, M., Yao, L., and Aubé, J. (2010). *J. Am. Chem. Soc.* 132: 2078–2084.

58 Zuo, Z., Xie, W., and Ma, D. (2010). *J. Am. Chem. Soc.* 132: 13226–13228.

59 Denzer, M. and Ott, H. (1969). *J. Org. Chem.* 34: 183–187.

60 (a) Beddoes, R.L., Davies, M.P.H., and Thomas, E.J. (1992). *J. Chem. Soc., Chem. Commun.* 538–540. (b) Baylis, A.M., Davies, M.P.H., and Thomas, E.J. (2007). *Org. Biomol. Chem.* 5: 3139–3155.

61 (a) Dolby, L.J. and Sakai, S. (1964). *J. Am. Chem. Soc.* 86: 1890–1891. (b) Dolby, L.J. and Sakai, S. (1967). *Tetrahedron* 23: 1–9.

62 Szostak, M. and Aubé, J. (2009). *J. Am. Chem. Soc.* 131: 13246–13247.

63 Yoshida, K., Sakuma, Y., and Ban, Y. (1987). *Heterocycles* 25: 47–50.

64 Schill, G., Löwer, H., Priester, C.U. et al. (1987). *Tetrahedron* 43: 3729–3745.

65 Ribelin, T.P., Judd, A.S., Akritopopulou-Zanze, I. et al. (2007). *Org. Lett.* 9: 5119–5122.

66 Fu, L., Xu, M., Yu, J., and Gutekunst, W.R. (2019). *J. Am. Chem. Soc.* 141: 2906–2910.

67 Xu, M., Bullard, K.K., Nicely, A.M., and Gutekunst, W.R. (2020). *Chem. Sci.* 10: 9729–9734.

68 Zhao, Q., Lalancette, R., Szostak, R., and Szostak, M. (2020). *ACS Catal.* 10: 737–742.